

## RESPONSE OF YIELDING STRUCTURES TO STATISTICALLY GENERATED GROUND MOTION

By Paul C. Jennings<sup>(1)</sup>

### SYNOPSIS

Artificial earthquake accelerograms are presented which possess the known properties of strong earthquake motion that are significant to the response of structures. Also developed is a general yielding force-deflection relation that describes hysteretic response varying between the limits of linear and elasto-plastic behavior. The response of simple yielding structures to earthquake motion is examined and a general hysteresis law for describing the response of yielding structures to earthquake acceleration is presented. Some statistics of the response of a member of the family of general yielding structures to an ensemble of eight artificial earthquakes are presented also.

### INTRODUCTION

The response of structures to strong earthquake ground motion has been an object of study in recent years at the California Institute of Technology. This paper summarizes the work done there by the author during the period 1960-1963. The technical details of the research are available<sup>(2,3,4,5)</sup> and interested readers are referred to these references for information not presented herein.

The studies consisted of three related efforts: 1) The construction of artificial earthquake accelerograms suitable for use in response studies; 2) The development of a general force-deflection relation to be used for describing the dynamic yielding behavior of structural elements and for approximating the force-deflection relation of actual structures from dynamic test results; and 3) An examination of the response of simple yielding structures to earthquake motion, including the formulation of a general hysteresis law and the calculation of statistics of the response of a particular yielding structure to an ensemble of artificial earthquakes.

The references at the section headings indicate sources of more detailed information for the topic of that section.

- 
1. Instructor, Department of Mechanics, United States Air Force Academy, Colorado.
  2. Housner, G.W. and Jennings, P.C., "Generation of Artificial Earthquakes" Proceedings of the American Society of Civil Engineers, Vol. 90 No. EM1 (Feb 64)
  3. Jennings, P.C., "Periodic Response of a General Yielding Structure" Ibid, (In Press, ASCE)
  4. Jennings, P.C. "Earthquake Response of a Simple Yielding Structure" (In Manuscript, to be submitted to the ASCE).
  5. Jennings, P.C. Response of Simple Yielding Structures to Earthquake Excitation, Pasadena; California Institute of Technology Earthquake Engineering Research Laboratory, (1963).

## EARTHQUAKE EXCITATION<sup>(2,5)</sup>

Several strong-motion earthquake accelerograms have been obtained on firm ground in the U.S.A. in recent years. Typically these accelerograms show a primary phase of strong motion lasting 15-25 sec, followed by a secondary phase of weaker motion that gradually dies away. Because the maximum response of a structure with damping is, in general, determined by the strong primary phase, it is customary to use only this phase in structural response studies. It is recognized upon examination of these recorded accelerograms that strong-motion earthquake acceleration is a statistical phenomenon.

Because of the statistical nature of the excitation, the information that can be obtained from response studies using a single earthquake record is limited and it would be desirable to have a large number of accelerograms of various intensities and durations. An ensemble of such artificial earthquakes could be used in structural response studies in place of the unavailable earthquake accelerograms. Because all the artificial accelerograms of an ensemble would be of the same length and intensity, the effects of these quantities could be separated from the effects due to changes of the structural parameters.

An ensemble of 8 artificial earthquake accelerograms of 30 sec duration have been generated. These records appear to possess individually, and on the average, the known pertinent properties of strong-motion earthquake accelerograms. The artificial earthquakes are 30 sec sections of a Gaussian random process with a power spectral density determined from an extension of an approximate theory developed by E. Rosenblueth and J.E. Bustamante.<sup>(6)</sup> The duration was chosen as 30 sec in order to model the acceleration of a very strong earthquake.

It is considered essential that the properties of any random process that is to be used for artificial earthquake accelerograms be compared to the known properties of strong-motion earthquakes. An accelerogram from the Taft, California earthquake of July 21, 1952 (Magnitude 7.7) is shown in Fig. 1, and in Fig. 2 are shown the accelerograms of two of the artificial earthquakes. Although no quantitative comparison is made from these figures, it is seen that the artificial accelerograms are qualitatively similar to the Taft record.

Fig. 3 shows the integrated velocity and displacement of the Taft accelerogram shown in Fig. 1.<sup>(7)</sup> The velocity and displacement of the artificial earthquakes were calculated in an identical manner and an example is shown in Fig. 4.

- 
6. Rosenblueth, E., and Bustamante, J.E., "Distribution of Structural Response to Earthquakes", Proceedings of the American Society of Civil Engineers, Vol. 88, No. EM3, (June 1962), pp. 75-106.
  7. Berg, G.V., and Housner, G.W., "Integrated Velocity and Displacement of Strong Earthquake Ground Motion", Bulletin of the Seismological Society of America, Vol. 51, No. 2, (April 1961), pp.175-189.

The velocity spectrum is the most useful known strong-motion earthquake statistic for the purposes of structural analysis. Because the velocity spectrum value is the maximum velocity obtained by a one degree of freedom structure in response to the ground motion, the spectrum value finds direct application in the analysis of simple, linear structures. Furthermore, normal mode techniques enable the response of multi-degree of freedom structures to be estimated. The velocity spectra of strong-motion earthquakes have been calculated<sup>(8)</sup>, and the average spectra are well known.<sup>(9)</sup> Fig. 5 shows the velocity spectra of the Taft accelerogram shown in Fig. 1, and the velocity spectra of one of the artificial earthquakes is given in Fig. 6. It is clear that the two sets of spectra are qualitatively similar. In these figures 'n' is the fraction of critical damping.

The velocity spectra of the artificial earthquakes were averaged and compared to a similar average for the recorded earthquake accelerograms. The results are shown in Fig. 7. It should be noted that the average earthquake spectra are smoothed versions of curves similar in appearance to those for the artificial earthquakes. The difference in the average undamped spectra is a consequence of the fact that the 30 sec duration of the artificial earthquakes was longer than the average duration of the strong-motion portions of the earthquake accelerograms.

That the duration of the excitation should have such an effect on the undamped spectra can be explained from energy considerations. The energy in an undamped structure builds up with time, whereas in a damped structure the energy tends to fluctuate about a mean value that is achieved, on the average, in several cycles of vibration of the structure. Thus for excitation longer than several periods of vibration of the structure, the duration of excitation has only a small effect on the average damped spectra.

To describe the effect of the excitation duration upon the average spectra and to characterize the influence of the natural period and damping upon the oscillation, an average velocity spectra formula has been developed

$$S_v = 1.796 \sqrt{\frac{\pi G(\omega)}{2n\omega} \left(1 - e^{-2n\omega t / 2.44}\right)} \quad (1)$$

where  $S_v$  is the average spectrum,  $\omega$  is the natural frequency of the structure,  $t$  denotes the duration of the earthquake accelerograms and  $G(\omega)$  is the power spectral density of the strong-motion phase of the acceleration. For the

- 
8. Alford, J.L., Housner, G.W., and Martel, R.R., Spectrum Analyses of Strong-Motion Earthquakes, Pasadena; California Institute of Technology Earthquake Research Laboratory, (1951).
  9. Housner, G.W., "Behavior of Structures During Earthquakes", Proceedings of the American Society of Civil Engineers, Vol. 85, No. EM4 (Oct. 1956), pp. 109-129.

U.S. accelerograms  $G(\omega)$  is given by

$$G(\omega) = \frac{0.01238 \left(1 + \frac{\omega^2}{147.8}\right)}{\left(1 - \frac{\omega^2}{242}\right)^2 + \frac{\omega^2}{147.8}} \quad (2)$$

This type of formula for  $G(\omega)$  was first proposed by H. Tajima<sup>(10)</sup> based on the work of K. Kanai.<sup>(11)</sup>

The comparison of the average spectra formula with the average spectra of strong-motion earthquakes is shown in Fig. 8. For this comparison the average duration of the strong-motion phase of the earthquakes was taken to be 18.6 sec. The comparison of the spectra formula with the spectra of the 30 sec artificial earthquakes is shown in Fig. 9.

It is concluded from the foregoing comparisons that the artificial earthquakes possess the known properties of strong-motion earthquakes that are significant for the purposes of structural analysis. By scaling the artificial earthquakes, ensembles of accelerograms can be produced which typify, approximately, certain past earthquakes. In order to determine appropriate scale factors it is necessary to measure the intensity of ground motion. Formerly the undamped spectrum intensity has been used for this purpose<sup>(8)</sup>, however, it was found that the acceleration r.m.s or the damped spectrum intensity are better measures of the strength of the ground motion than is the undamped spectrum intensity.

Table I shows some properties of eight strong-motion earthquake accelerograms. The scale factor given for each earthquake is the number by which the artificial earthquakes should be multiplied to produce an ensemble with the same r.m.s acceleration as that earthquake. For example, if the artificial earthquakes are multiplied by 2.9, the resulting accelerograms will have an average r.m.s value equal to the average for the two components of the El Centro 1940 shock. The velocity spectra and, presumably, the results of other structural investigations using these accelerograms will be approximately the same statistically as if an ensemble of records of the strength of El Centro 1940 had been used. It is in this manner that the artificial earthquakes can be used in studying the earthquake response of complex structures or as standard ground motions for the design of structures.

- 
10. Tajima, H., "A Statistical Method of Determining the Maximum Response of a Building Structure During an Earthquake", Proceedings of the Second World Conference on Earthquake Engineering, Vol. II, Tokyo and Kyoto, Japan, (July 1960).
  11. Kanai, K., "Semi-empirical Formula for the Seismic Characteristics of the Ground", Bulletin of the Earthquake Research Institute, University of Tokyo, Vol. 35, (June 1957), pp. 309-325.

## A GENERAL YIELDING STRUCTURE<sup>(3,5)</sup>

In the large majority of earthquake response studies where yielding has been considered, the elasto-plastic or bilinear hysteretic force-deflection relations have been used to describe the nonlinearity of the restoring elements. These relations have been used chiefly because of their simplicity; it is expected that most structures would not exhibit the sharp departure from linearity that these relations possess, but would show instead a more rounded force-deflection relation.

Because of the necessity of considering some degree of yielding in the response of structures to strong earthquake motion, it would be desirable to have available a general force-deflection relation that describes yielding varying between the limits of elasto-plastic and linear behavior. One such general relation is shown in Fig. 10.

The skeleton curve describes the force deflection relation when the magnitude of the load is increased from zero. For this general yielding relation the skeleton curve is described by

$$\frac{x}{x_y} = \frac{p}{p_y} + \alpha \left( \frac{p}{p_y} \right)^r \quad (3)$$

where  $x$  is the displacement,  $x_y$  denotes a characteristic displacement value,  $p$  is the force,  $p_y$  represents a characteristic force,  $\alpha$  is a positive constant, and  $r$  is a positive odd integer greater than unity. This type of formulation was first used by Ramberg and Osgood<sup>(12)</sup> to describe stress-strain curves. The hysteresis loop is given by

$$\frac{x - x_i}{2x_y} = \frac{p - p_i}{2p_y} + \alpha \left( \frac{p - p_i}{2p_y} \right)^r \quad (4)$$

in which the point  $\left( \frac{x_i}{x_y}, \frac{p_i}{p_y} \right)$ , the origin of the curve, is the most recent point of loading reversal.

The generality of the force-deflection relation is achieved by varying the constants  $r$  and  $\alpha$ ; this generality is illustrated in Figs. 11 and 12. In Fig. 11 the value of  $r$  is constant and  $\alpha$  is varied whereas in Fig. 12  $\alpha$  is constant and  $r$  is varied. From these figures and from equations 3 and 4 it can be seen that linear behavior is approached as  $\alpha$  tends to zero and that elasto-plastic behavior is approached as  $r$  tends to infinity.

---

12. Ramberg, W., and Osgood, W.R., "Description of Stress-Strain Curves by Three Parameters", NACA TN 902, (July 1943).

The steady-state response to sinusoidal excitation is a common dynamic test result and therefore, in order to make comparisons with results from actual structures, it would be advantageous to have similar theoretical results for the general yielding structure. Fig. 13 illustrates one result of the steady-state response of the general yielding structure to sinusoidal excitation. This figure gives the resonant steady-state amplitude in response to the force  $F_0 \sin \omega t$  as a function of the force level  $F_0/p_y$ . Also shown on this figure are similar curves for some damped linear structures. It should be noted that the resonant frequencies of the structures shown in Fig. 13 are not necessarily the same in view of the change of resonant frequency with amplitude exhibited by the nonlinear structures.

Frequency response curves for several examples of the general yielding structure are shown in Fig. 14. The variation of the general structure from linear to elasto-plastic behavior is clearly evident in this figure. To verify the theoretical results, a typical family of frequency response curves have been verified by numerical integration of the equation of motion.

By making an energy balance the equivalent viscous damping factor for steady-state response of the general yielding structure can be determined. The maximum value that this factor can assume for a particular structure is

$$n_{eq}(\text{max.}) = \frac{1}{2\pi} \left( \frac{r-1}{r+1} \right) \quad (5)$$

The maximum equivalent damping factor is characterized in Fig. 13 by the line from the origin that is tangent to the curve for a yielding structure. The maximum possible value of the equivalent viscous damping factor occurs for the elasto-plastic structure and is  $1/2\pi = 0.159$  of critical. In view of the generality of the yielding relation, it appears unrealistic in earthquake response studies to assign viscous damping factors greater than  $1/2\pi$  to the effects of yielding in structures of the softening type.

The general yielding structure was developed for use in earthquake studies and to provide a means for determining the dynamic force-deflection relation of a structure from the results of sinusoidal excitation tests. Towards this latter purpose the variation of natural frequency with amplitude and excitation level, the frequency response curves, and the variation of the equivalent viscous damping factor with amplitude are the results that would be of the greatest value in determining a nonlinear force-deflection relation that approximates the dynamic behavior of the structure. In cases where viscous damping as well as yielding is operative, small amplitude tests can be made to find the viscous damping factor which can be subtracted from equivalent damping factors determined at higher amplitude levels to find the damping factor associated with yielding.

Some preliminary studies indicate that the general yielding structure may find successful application in modeling actual structural behavior, but there is a lack of experimental data for dynamic response of structures in or near the yielding range.

## RESPONSE TO EARTHQUAKE EXCITATION<sup>(4,5)</sup>

When a simple yielding structure responds to strong earthquake motion, the force-deflection relation is no longer the simple hysteresis loop that describes steady-state response to sinusoidal excitation. In the cases of the elasto-plastic and bilinear hysteretic structures, the yielding relations for general excitation are not complex and are well known. The general yielding structure discussed above, however, requires the formulation of a more general hysteresis law.

A class of yielding structures can be defined that includes the general yielding structure as well as the linear, elasto-plastic, and bilinear hysteretic structures. This class of yielding structures is determined by the geometry of the hysteresis curves, and by the hysteresis law that governs their response.

The application of the hysteresis law is best introduced by the examples for the general structure shown in Fig. 15. Part A of this figure shows the response to an alternating force of increasing magnitude; Part B illustrates the response to a load that increases, then decreases to less than zero, and then increases again, etc. Part C shows how the hysteretic curves could reduce to a loop in response to periodic excitation, and the response to some general force is illustrated by part D. The dashed lines in Fig. 15 are the skeleton curves.

With the help of the curves shown in Fig. 15 it can be seen that the following definitions are useful in describing yielding behavior.

1. The minimum curve (min curve) is that ascending curve whose intercept on the  $x/x_y$  axis is less than that for all previous ascending curves and whose origin, the minimum point (min point), has a value of  $x/x_y$  less than that for all previous ascending curves. The first minimum curve is the skeleton curve with origin and intercept at (0,0).
2. The maximum curve (max curve) is that descending curve whose intercept on the  $x/x_y$  axis is greater than that for all previous descending curves and whose origin, the maximum point (max point), has a value of  $x/x_y$  greater than that for all previous ascending curves. The first maximum curve is also the skeleton curve.
3. The upper boundary is the min curve between its least and greatest points of contact with the skeleton curve and is the skeleton curve elsewhere.
4. The lower boundary is the max curve between its least and greatest points of contact with the skeleton curve and is the skeleton curve elsewhere.

Employing these definitions, the hysteresis law for the class of yielding structures discussed herein can be stated:

Force-deflection values are given by a hysteretic curve originating from the point of most recent loading reversal until either the upper or lower boundary is contacted. Thereafter the force-deflection values are given by that boundary until the direction of loading again is reversed.

The cases shown in Fig. 15 are examples of the application of the hysteresis law to the general yielding structure.

In addition to obeying the hysteresis law, the class of structures is restricted to those softening systems for which the skeleton curve is symmetric about the origin and for which the hysteretic curves are geometrically similar to, but twice as large as, the skeleton curves. This requirement is met by scaling the parameters of the hysteretic curves to be exactly half those of the skeleton curves.

It is not difficult to show that this class includes the linear, elastoplastic, and bilinear hysteretic structures. In the case of the general yielding structure, the skeleton curve is given by equation 3 and all other hysteretic curves are given by equation 4. The application of the hysteresis law to the general structure is chiefly a process of determining the upper and lower boundaries as the structure responds to the earthquake.

It is thought that a reasonable approximation to the dynamic behavior of many actual structures can be achieved by the use of the general yielding structure and the hysteresis law, but insufficient experimental data are available to verify this conclusion.

#### EQUATION OF MOTION AND ENERGY EQUATION (4,5)

The equation of motion of a single degree of freedom yielding structure in response to earthquake excitation can be written as

$$\frac{\ddot{x}}{x_y} + 2n\omega_o \frac{\dot{x}}{x_y} + \omega_o^2 \frac{p}{p_y} \left( \frac{x}{x_y} \right) = -\omega_o^2 \frac{\ddot{y}}{q_y} \sigma(t) \quad (6)$$

where  $n$  is the fraction of critical damping.  $\omega_o$  denotes the natural frequency of small oscillations, and  $p/p_y$  is a function of  $x/x_y$ . The variable  $q_y = p_y/m$  and, if  $p_y$  is the yield strength of the structure,  $q_y$  is commonly called the yield level, the acceleration of the foundation that will develop the yielding force  $p_y$  in the resisting elements of the structure. The intensity of the earthquake acceleration is measured by  $\ddot{y}$ , and  $\sigma(t)$  is the dimensionless time record of the excitation. Different earthquakes will have varying  $\ddot{y}$  values, but in each case  $\sigma(t)$  will be a dimensionless accelerogram with an intensity of unity.

By letting  $\tau = \omega_o t$ , the frequency dependence of the left side of equation 6 can be removed yielding

$$\frac{x''}{x_y} + 2n \frac{x'}{x_y} + \frac{p}{p_y} \left( \frac{x}{x_y} \right) = -\frac{\ddot{y}}{q_y} \sigma(\tau/\omega_o) \quad (7)$$



where the primes denote differentiation with respect to  $\tau$ . This form of the equation of motion was used for numerical evaluation of earthquake response.

Equations 6 and 7 describe the response of a simple yielding structure in terms of the variable  $x/x_y$ , the ratio of the deflection to the characteristic deflection. For application to an elasto-plastic or bilinear hysteretic structure  $x_y$  and  $p_y$  are the yield displacement and force, respectively, and  $q_y$  is the yield level. When equations 6 and 7 are used to describe the general yielding structure,  $x_y$  and  $p_y$  are characteristic values subject to the restriction that  $p_y/x_y$  be the slope of the skeleton curve near the origin. For large values of  $r$  the knee of the skeleton curve of the general structure is well-defined and since  $p_y$  and  $x_y$  are near this knee they can be referred to as yield values without misinterpretation. If  $r$  is not large the departure from linearity of the skeleton curve is gradual and  $p_y$  (or  $x_y$ ) can be chosen more arbitrarily. For example,  $p_y$  could be the force at which the departure from linearity is 10% of the total deflection.

In the case of a linear structure  $p/p_y = x/x_y$  and equations 6 and 7 can be simplified. The equations also can be simplified somewhat in the special case where  $p/p_y$  is an algebraic function of  $x/x_y$ .

It is seen from examination of equations 6 and 7 that it is the ratio  $\ddot{y}/q_y$  that determines the relative strength of the excitation. This implies that the effect on the response of a structure produced by doubling the acceleration intensity  $\ddot{y}$  can be achieved also by halving the yield level  $q_y$ . Thus the response, as measured by  $x/x_y$ , of a simple yielding structure with a yield level of .10 g to an earthquake of the strength of El Centro 1940 would resemble that of a .20 g structure in response to an earthquake twice as strong as the El Centro shock.

Table II shows the values of  $\gamma = \ddot{y}/q_y$  for several strong-motion earthquakes and for several yield levels. The values of  $\ddot{y}$  used in the table are the average acceleration r.m.s values of the two components of the shock and are taken from table I.

The response of a structure to earthquake excitation is identical to that of a structure on an immovable foundation excited by the force  $-m\ddot{y}(t)$ , where  $m$  is the mass of the structure and  $\ddot{y}(t)$  is the ground acceleration. By considering the work done by this force as the structure moves through an incremental deflection the energy equation for the structure can be found. In a convenient dimensionless form this equation is

$$\frac{E_I}{\frac{1}{2}x_y p_y} = \left(\frac{x'}{x_y}\right)^2 + 4n \int_0^\tau \left(\frac{x'}{x_y}\right)^2 d\tau + 2 \int_0^\tau \left(\frac{x'}{x_y}\right) \frac{p}{p_y} d\tau \quad (8)$$

where  $E_I$  is the energy supplied to the structure since the beginning of the earthquake. If  $p_y$  and  $x_y$  are yield values, the left side of equation 8 is the ratio of the energy input to that energy which can be stored elastically in the structure. The first term on the right side is the kinetic energy,

the second term gives the energy dissipated by viscous friction, and the third term contains both the energy dissipated by yielding and the potential energy in the restoring elements of the structure. For a linear structure  $p/p_y = x/x_y$  and in this case the last term can be integrated to produce the potential energy.

The above energy equation is in terms of the relative displacement and velocity of the structure rather than the absolute values of these quantities. Because it is the relative values of displacement and velocity that are important for design, it is thought that an energy analysis in terms of relative motion is more meaningful than one in terms of absolute motion. It is noted also that the integrals in equation 8 are all taken with respect to time, a fact that simplifies the numerical evaluation of these integrals.

#### RESPONSE TO EARTHQUAKE MOTION<sup>(4,5)</sup>

To illustrate the use of the general yielding structure and the artificial earthquake accelerograms in earthquake response studies, the yielding structure given by  $\alpha = 0.10$  and  $r = 9$  was subjected to an ensemble of eight artificial earthquakes. The structure selected has a well-defined knee in the skeleton curve and  $x_y$  and  $p_y$  are referred to as the yield deflection and force, respectively. Similarly,  $q_y$  is called the yield level. The skeleton curve and some hysteresis loops for  $\alpha = 0.10$  and  $r = 9$  are shown in Fig. 16.

In the calculation the acceleration ratio  $\gamma = \ddot{y}/q_y$  was given the values 0.25, 0.50, 0.75 and 1.00. (cf. Table II). Four values of viscous damping factors were used: 0, 0.02, 0.05 and 0.10. Because the average velocity spectra for the linear structure are relatively smooth when damping is present, it is expected that the average of the spectra of the yielding structure also will be smooth and therefore can be determined by a small number of natural periods. The natural periods of small oscillations used in the calculations were 0.5, 1.0, 1.5, 2.0 and 2.5 sec. Only partial results of the calculations are presented here.

Average displacement spectra were obtained by averaging the maximum displacement for each of the eight artificial earthquakes. Fig. 17 shows the average maximum displacement values for  $n = 0$  and  $n = 0.02$ . The range of the values determining the averages for zero damping are shown in Fig. 18. Judging from the uniform spacing of the average spectra and from the moderate range of the individual values, it is concluded the eight accelerograms are adequate for determining the average spectra. It is seen from these averages that for a constant acceleration ratio  $\ddot{y}/q_y$ , the expected value of  $x/x_y$  increases as the period decreases. If  $\ddot{y}$  and  $q_y$  are both constant, this implies that structures with smaller periods will experience greater deflections as measured by  $x/x_y$ . Because an infinitely stiff structure would experience no relative displacement, the value of  $x$  must approach zero as the natural period approaches zero. But the yield displacement  $x_y$  also approaches zero as the natural period approaches zero so that the overall effect is for stiff structures to yield relatively more than do flexible structures with the same yield level, as is shown in Fig. 17.

As might be expected, the addition of small amounts of viscous damping decreases both the average and the range of the data but does not affect the general character of the spectrum averages.

Equation 8 was used to determine the energy imparted to the structure during the earthquake. The energy input varies little with a change of viscous damping and Fig. 19 shows the average energy input spectra as a function of the acceleration ratio for  $n = 0.10, 0.05, 0.02,$  and  $0$ . The structure can contain elastically an average ratio of near unity, so energy input greater than unity must be dissipated by viscous damping or by yielding. It is seen that structures with lower periods will receive, and therefore must dissipate, relatively more energy than more flexible structures.

For linear structures the energy input increases as the square of the acceleration intensity, and an interesting comparison can be made by multiplying the energy input for  $\gamma = 0.25$  by 16 and comparing with the input for  $\gamma = 1.0$ , as is done in Fig. 19. Because the structural response for  $\gamma = 0.25$  is nearly linear, the comparison reinforces G.W. Housner's assumption that the energy imparted by an earthquake to a nonlinear structure is approximately equal to that received by a linear structure with the same natural period.

Energy dissipated by viscous damping does not entail structural damage as a rule, whereas energy dissipated by yielding, especially if large, must be accompanied by some structural damage and perhaps failure. Therefore, a useful statistic for structural response is the relative amounts of energy dissipated by viscous damping and by yielding. This result for  $n = 0.02$  is shown in Fig. 20 in which  $E_p$  is the energy dissipated by yielding and  $E_v$  that dissipated by viscous damping. Because all the energy is dissipated by viscous damping in a linear structure, it is seen from Fig. 20 that an increase in period results in more nearly linear behavior.

To illustrate the use of these results in analysis of earthquake response, a simple example is presented. It is assumed that the one degree of freedom structure to be studied has yielding behavior approximated by  $r = 9$  and  $\alpha = 0.10$ . The natural period of the structure is 1 sec, the damping is 0.02 and the yield level is 0.10 g. Information about the response to earthquakes of the strength of El Centro 1940 is sought. From table II it is found that the acceleration ratio is 0.62, and from Fig. 17 it is seen that the expected maximum displacement is about three times the yield displacement. Fig. 19 indicates an energy input near 40 times what can be contained elastically and from Fig. 20 it is expected that 1/4 of this energy would be dissipated by viscous damping and the remainder by yielding. As can be seen from the figures, more nearly linear behavior of the structure could be achieved at the same yield level by lengthening the period. More nearly linear behavior could be achieved also by increasing  $q_y$ , thereby lowering the acceleration ratio  $\ddot{y}/q_y$ .

## RESULTS AND CONCLUSIONS

The more important results and conclusions are listed below:

- 1) It is concluded from the comparison of the properties of the real and artificial earthquakes that the artificial accelerograms possess the known properties of strong motion earthquakes pertinent to structural analysis.
- 2) From the ability of the general yielding structure to describe yielding varying between the limits of linear and elasto-plastic behavior it is concluded that this relation may be useful in determining the dynamic force-deflection relations of actual structures from sinusoidal shaking tests.
- 3) It was found that the maximum possible equivalent viscous damping coefficient for the general yielding structure was  $1/2\pi$  of critical. In view of the generality of the yielding relation, it is concluded that it may be unrealistic to attribute damping coefficients greater than this to the effects of yielding.
- 4) If the response is measured in terms of  $x/x_y$  it was found that the ratio  $\ddot{y}/q_y$  determines the relative strength of the earthquake excitation for simple structures.
- 5) From the response studies for the structure given by  $\alpha = 0.10$  and  $r = 9$  it is concluded that the artificial earthquakes can be useful for approximating the statistics of response in the analysis and design of aseismic structures.

## ACKNOWLEDGEMENTS

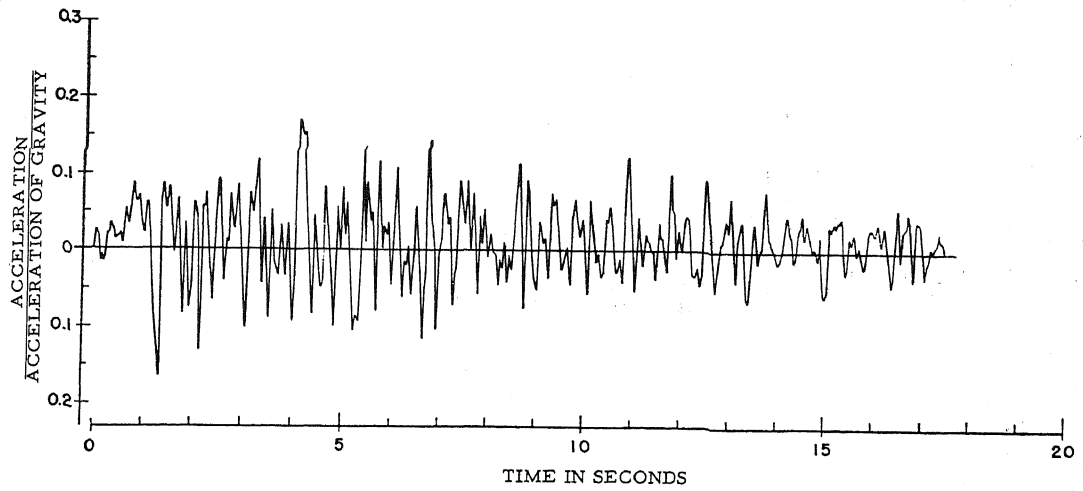
The writer is indebted to Professor G. W. Housner for his guidance and assistance throughout these studies. The advice and help of Professors D. E. Hudson, T. K. Caughey and J. N. Franklin are appreciated also.

TABLE I  
Strong-Motion Earthquake Properties

Earthquake Accelerogram	Magnitude	Estimated Strong-Motion Duration	Component	Acceleration r.m.s. ft/sec <sup>2</sup>	Average r.m.s	Scale Factor
El Centro, Calif. May 18, 1940	7.1	25 sec	N.S. E.W.	2.20 1.82	2.01	2.9
Olympia, Wash. April 13, 1949	7.1	21	S80°W S10°E	1.95 1.57	1.76	2.5
Taft, Calif. July 21, 1952	7.7	14	S69°E N21°E	1.45 1.42	1.44	2.1
El Centro, Calif. Dec 30, 1934	6.5	17	N.S. E.W.	1.43 1.27	1.35	1.9

TABLE II  
Earthquake Acceleration Ratios

Earthquake Accelerogram	$\ddot{y}$	$q_y = 0.03g$	$q_y = 0.05g$	$q_y = 0.10g$	Acceleration Ratio $\gamma = \ddot{y}/q_y$ $q_y = 0.20g$
El Centro, Calif. May 18, 1940	2.01	2.1	1.2	0.62	0.31
Olympia, Wash. April 13, 1949	1.76	1.8	1.1	0.55	0.27
Taft, Calif. July 21, 1952	1.44	1.5	0.89	0.45	0.22
El Centro, Calif. Dec 30, 1934	1.35	1.4	0.84	0.42	0.21



ACCELEROGRAM FOR THE TAFT, CALIF. EARTHQUAKE OF JULY 21, 1952. COMPONENT S69<sup>0</sup>E.

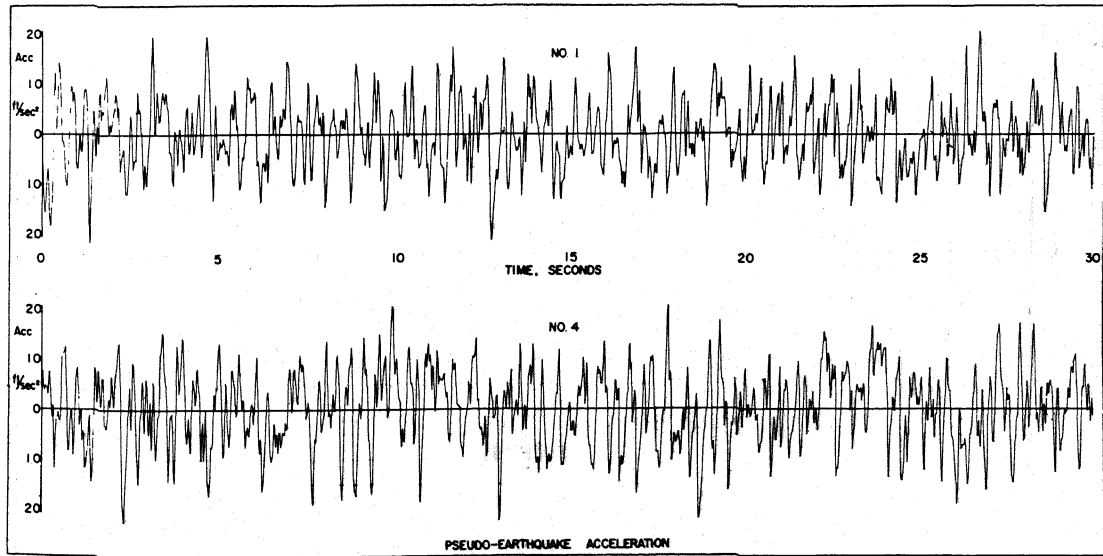


FIG. 2 ACCELEROGRAMS OF ARTIFICIAL EARTHQUAKES NOS. 1 AND 4.

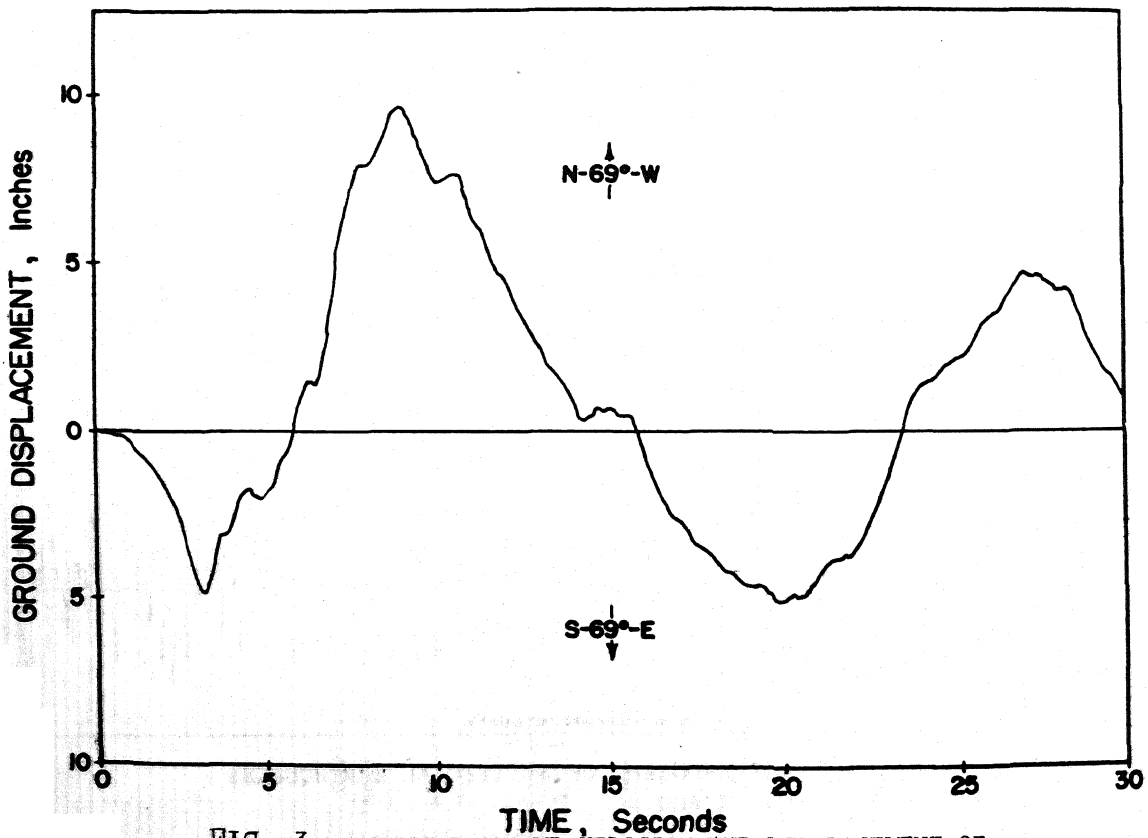
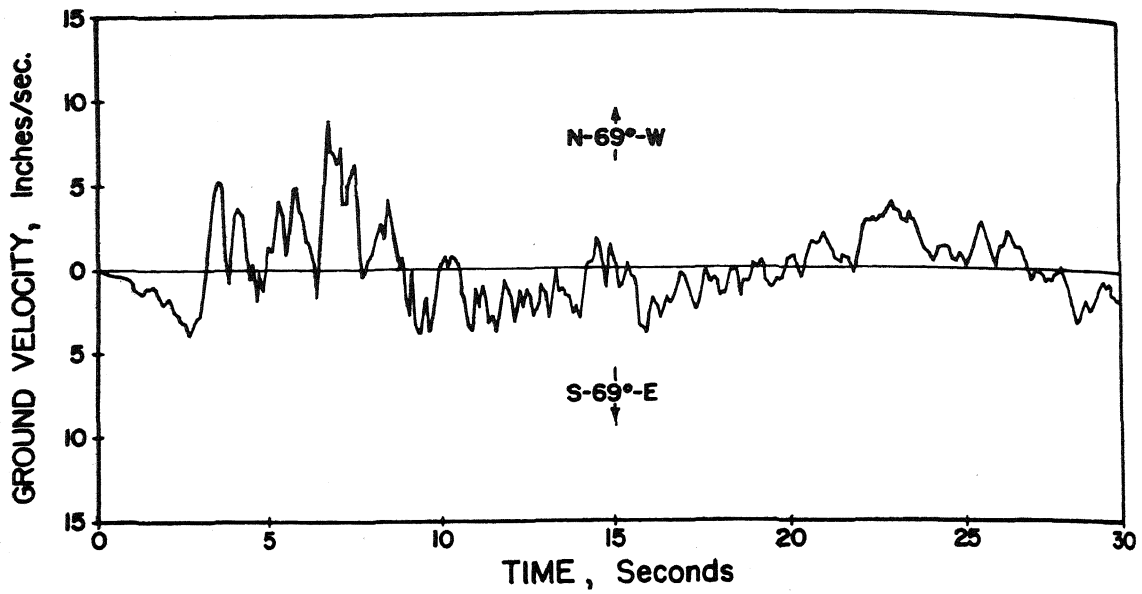


FIG. 3 INTEGRATED GROUND VELOCITY AND DISPLACEMENT OF THE TAFT, CALIF. EARTHQUAKE OF JULY 21, 1952. COMPONENT S69°E.



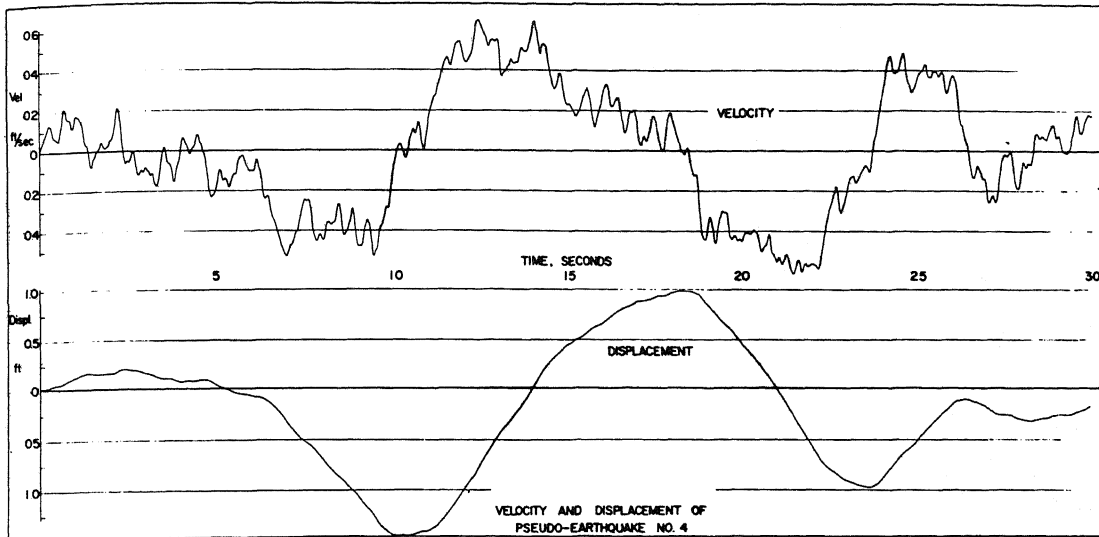


FIG. 4 INTEGRATED GROUND VELOCITY AND DISPLACEMENT OF ARTIFICIAL EARTHQUAKE NO. 4.

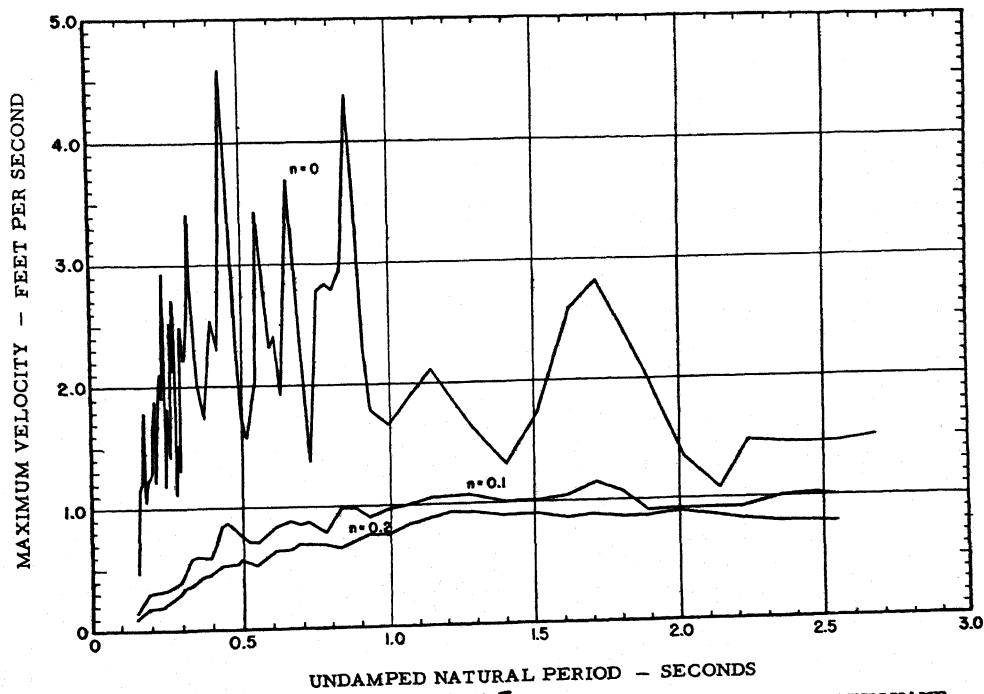
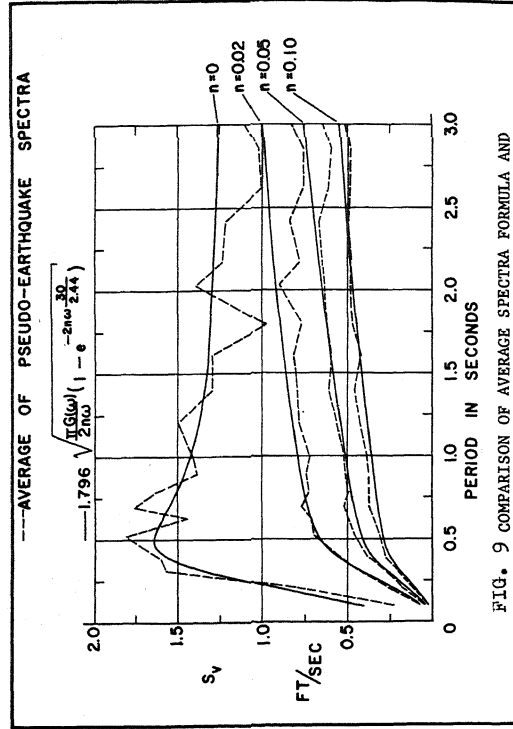
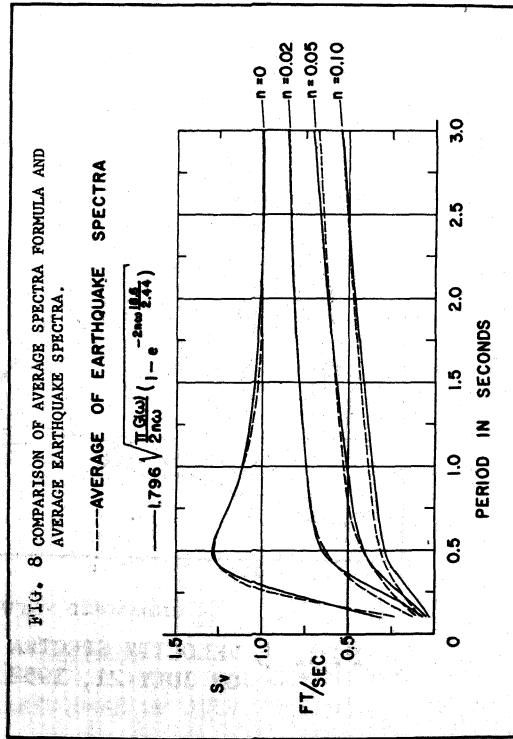
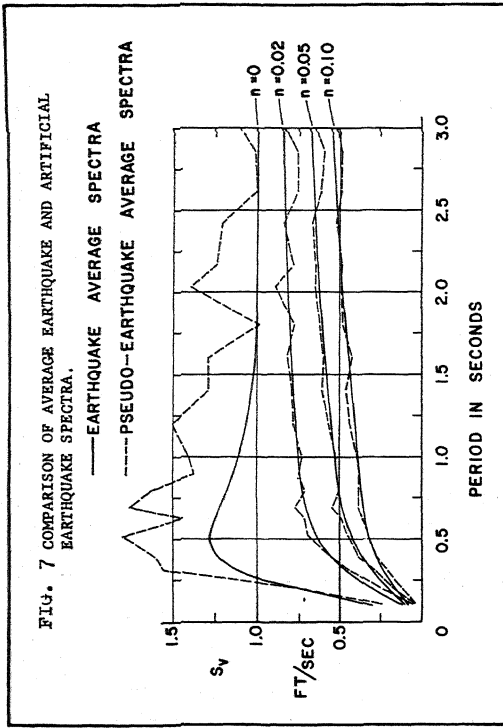
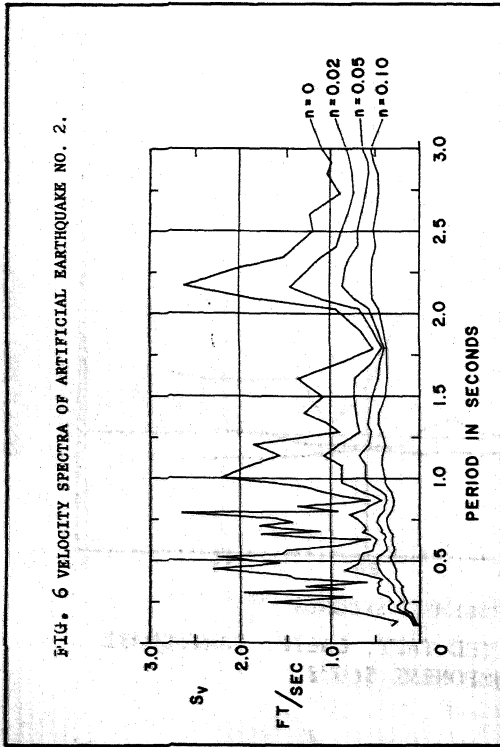


FIG. 5 VELOCITY SPECTRA FOR THE TAFT, CALIF. EARTHQUAKE OF JULY 21, 1952. COMPONENT S69<sup>0</sup>E.



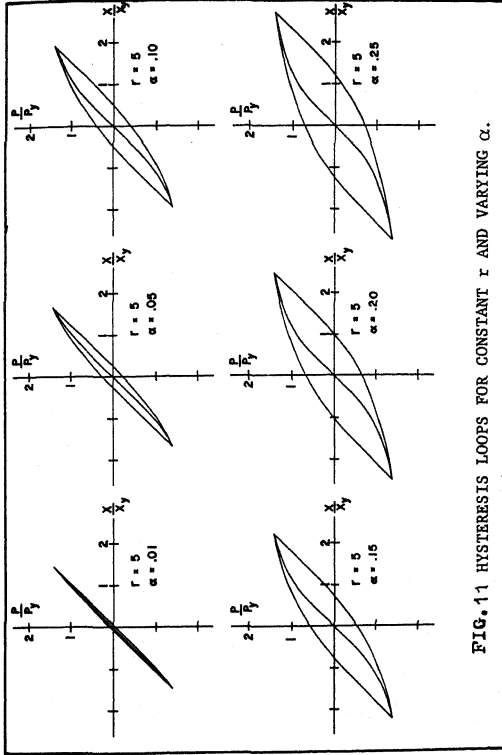


FIG. 11 HYSTERESIS LOOPS FOR CONSTANT  $r$  AND VARYING  $\alpha$ .

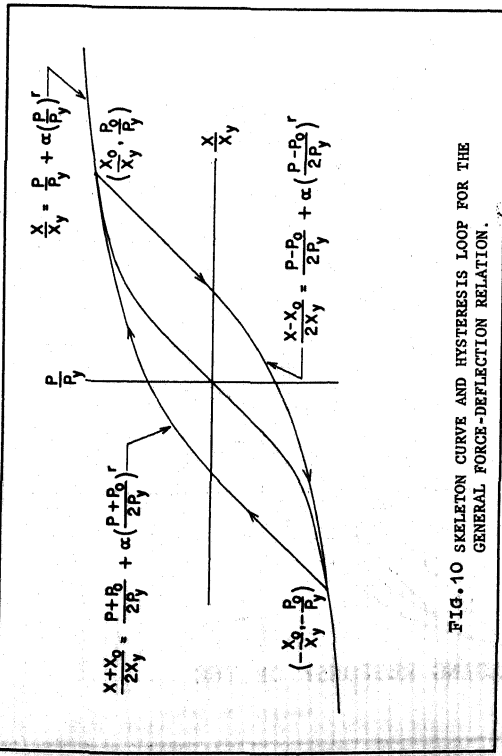


FIG. 10 SKELETON CURVE AND HYSTERESIS LOOP FOR THE GENERAL FORCE-DEFLECTION RELATION.

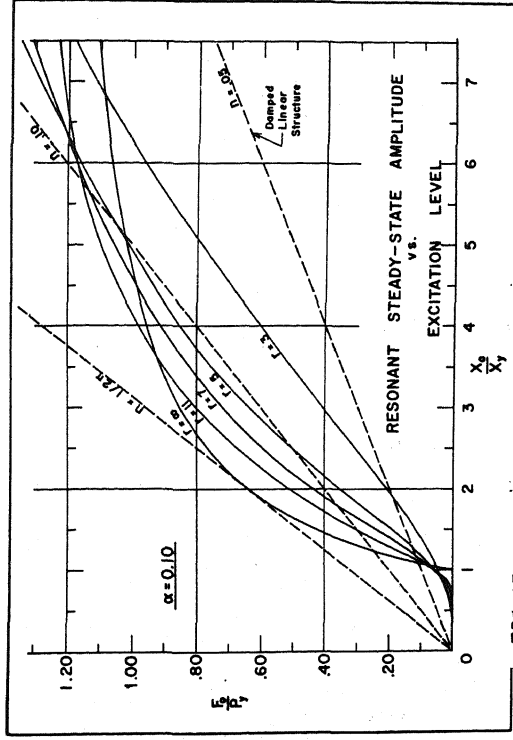


FIG. 13 RESONANT STEADY-STATE AMPLITUDE OF THE GENERAL YIELDING STRUCTURE IN RESPONSE TO  $F_0 \sin \omega t$ .

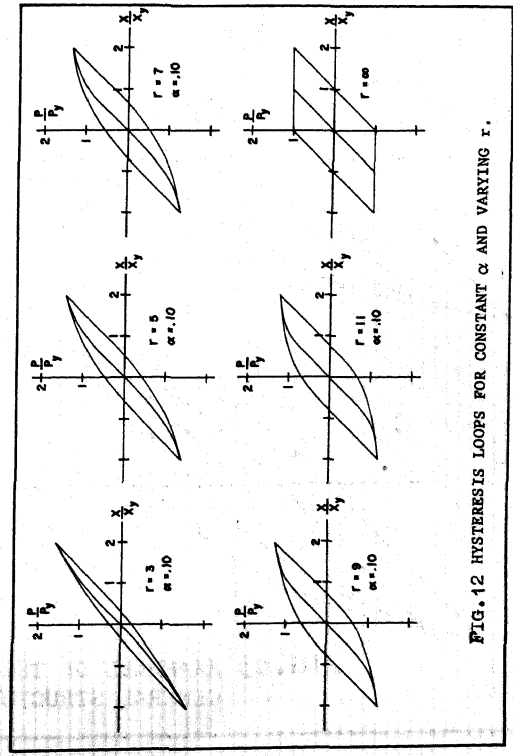


FIG. 12 HYSTERESIS LOOPS FOR CONSTANT  $\alpha$  AND VARYING  $r$ .

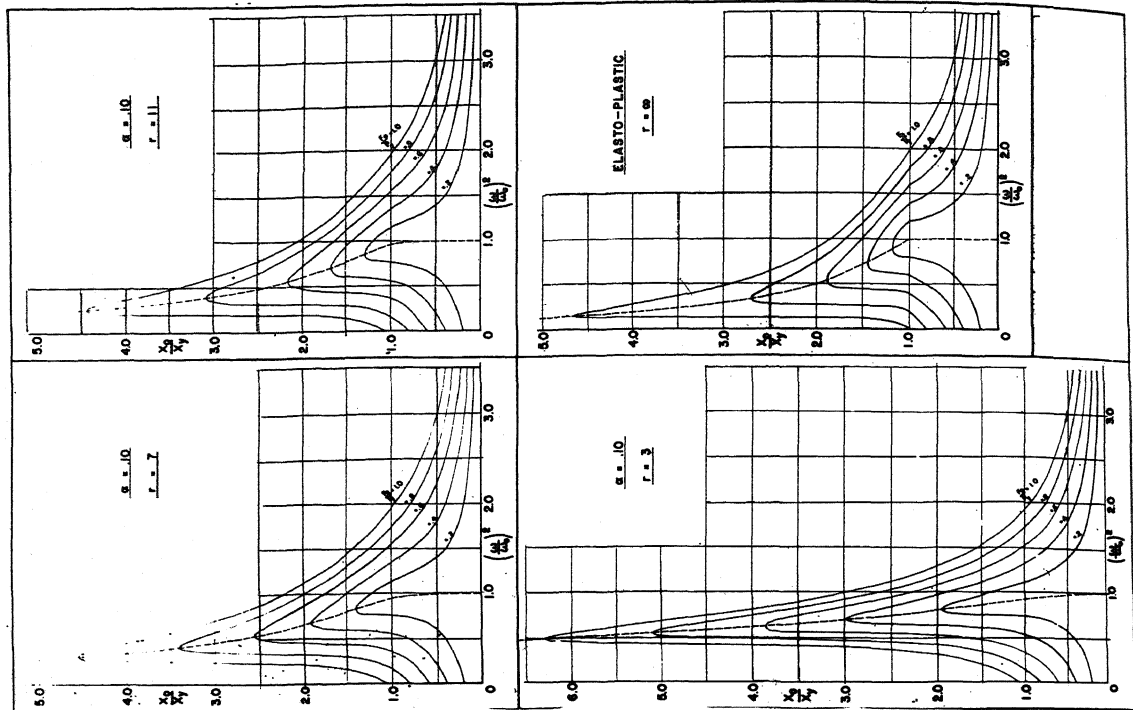


FIG. 14 FREQUENCY RESPONSE CURVES FOR THE GENERAL YIELDING STRUCTURE

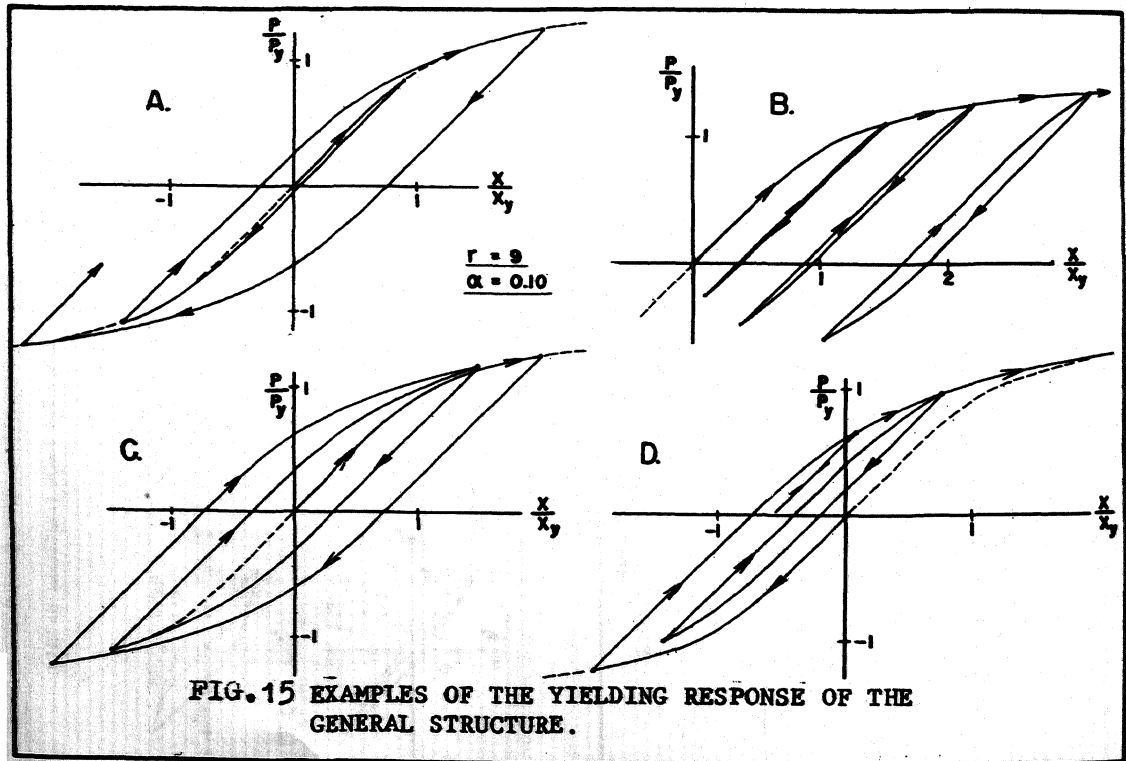


FIG. 15 EXAMPLES OF THE YIELDING RESPONSE OF THE GENERAL STRUCTURE.

RESPONSE OF YIELDING STRUCTURES TO STATISTICALLY GENERATED GROUND MOTION  
BY P.C. JENNINGS

QUESTION BY: C. MACKINTOSH - U.S.A.

On figures 17 and 19 the author comments on page 11 that the energy multiplies up to 40 times. Is that assuming zero damping?

AUTHOR'S REPLY: In the preparation of Fig. 19 it was found that the fraction of critical damping of the structure had very little effect on the amount of energy input when compared to the effects of natural period and acceleration ratio. Therefore all four values of damping considered in the study (0, 0.02, 0.05 and 0.10) were averaged in constructing the energy input curves shown in Fig. 19.

QUESTION BY: D.S. CARDER - U.S.A.

Waves of about 15 second period are observed in ground displacements found from integration of accelerograms obtained from instruments with a period of 0.1 sec. or less. Are not these waves of a random nature?

AUTHOR'S REPLY: Yes, in addition to what long-period components may have been in the actual earthquake acceleration, the long-period waves in the integrated displacements of real earthquakes are relatively sensitive to instrument error and to human error in digitizing the acceleration record. However, the random behaviour of the displacements obtained from the artificial earthquake records, in which these errors were not present, indicates that long-period motions of a statistical nature may not be unreasonable for actual ground motions.

QUESTION BY: J.I. BUSTAMANTE - MEXICO

Regarding the presentation, I would like to emphasize that the geology is implicitly included in the power spectral density used to generate the artificial earthquakes. One certainly will not use this power spectral density for all subsoil conditions.

AUTHOR'S REPLY: This is true; in this case, the power spectral density was determined from records recorded on firm alluvium at relatively short epicentral distances. It is important to note, however, that considering the eight artificial earthquakes as a group, local geology is not a variable since they are all generated from the same random process. The variations of the velocity spectra, ground velocities and ground displacements of the artificial earthquakes (see reference 2) are due entirely to the random nature of the accelerograms.

This suggests that the variations observed in velocity spectra, etc. found from real earthquake motions recorded on similar soil conditions may be due to the random character of earthquake acceleration, rather than to varying conditions of local geology.